Microscopic Basis of Magnetism

Magnetism of Insulators Metals and Things-In-Between

Figures and Illustrations

Sriram Shastry

IISc, Bangalore, India

Random Phase approximation: Gell Mann Brueckner Sawada 1958-59. Inverse susceptibility as a function of r_s

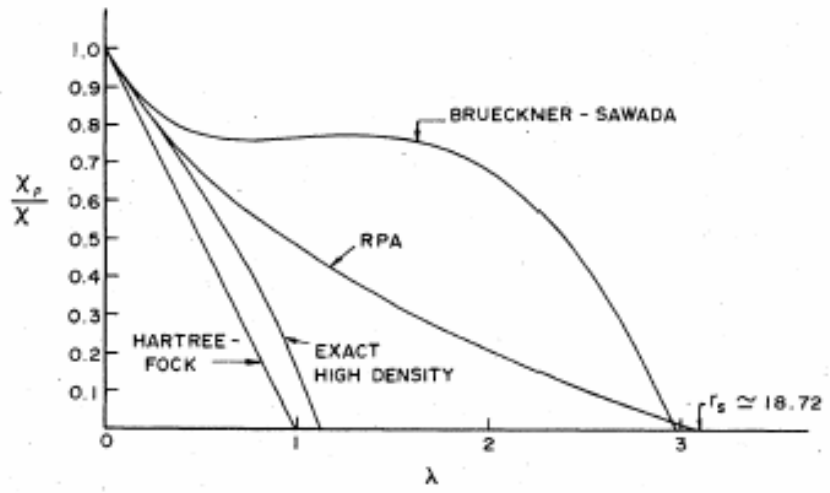

FIG. 1. Inverse susceptibility for various values of $\lambda(=r_s/6.029)$. The curve marked Brueckner-Sawada is from Ref. 15 [see Eq. (1.1.)]. The curve marked "exact high density" is a result of this work where we have corrected one of the two terms obtained by BS [see Sec. III, Eq. (3.32)]. The RPA curve is obtained from a computation of Eq. (2.39).

l =r_s/6.03

Curve from SS Phys Rev B17, 385(1978).

RPA predicts PM metal for rs ~ 18!

In[5]:=
```
e@rs_, x_D =
  2.21 ê rs^2 HH1 + xL^H5 ê 3L + H1 - xL^H5 ê 3LL -
   .916 HH1 + xL^H4 ê 3L + H1 - xL^H4 ê 3LL ê rs
```

Out[5]=
$$-\frac{0.916\ \text{HH1} - \text{xL}^{4\hat{e}3} + \text{H1} + \text{xL}^{4\hat{e}3}\text{L}}{\text{rs}} + \frac{2.21\ \text{HH1} - \text{xL}^{5\hat{e}3} + \text{H1} + \text{xL}^{5\hat{e}3}\text{L}}{\text{rs}^2}$$

In[30]:=
```
Plot@8e@5, xD, e@5.5, xD, e@6, xD<,
  8x, 0, 1<D
```

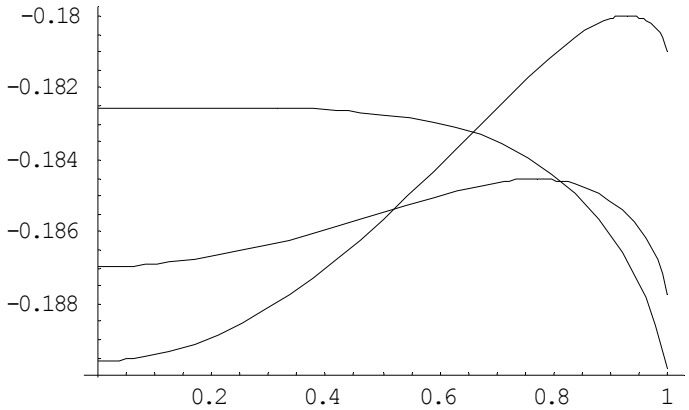

Out[30]= ¦ Graphics ¦

In[32]:=
```
Plot@e@rs, 0D - e@rs, 1D, 8rs, 4, 6<D
```

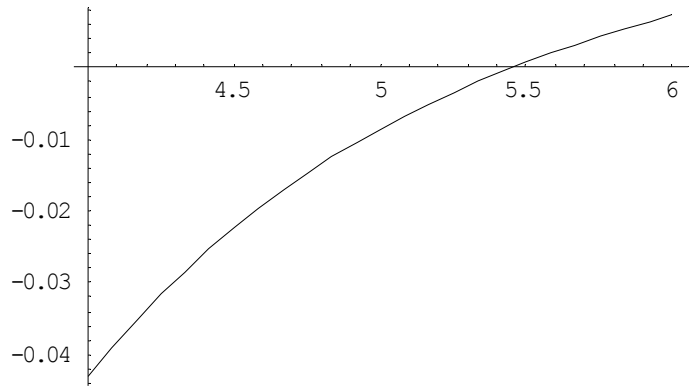

Out[32]= ¦ Graphics ¦

PHYSICAL REVIEW B VOLUME 18, NUMBER 7 1 OCTOBER 1978

Ground state of the fermion one-component plasma: A Monte Carlo study in two and three dimensions

D. Ceperley*
Laboratoire de Physique Theorique et Hautes Energies, Université de Paris XI, Orsay, France
(Received 26 April 1978)

We have performed fermion Monte Carlo variational calculations to determine the equation of state of the uniform electron one-component plasma in two and three dimensions. The ground-state excess energies calculated by the Monte Carlo method are very precise and in agreement with those of other calculations in the metallic density range and in the very-low-density Wigner crystals. Three phases have been investigated: the Wigner crystal, the normal or unpolarized fluid, and the polarized fluid. The Wigner crystal has the lowest energy for $r_s > 67$ in three dimensions and $r_s > 33$ in two dimensions. The totally polarized quantum fluid is stable for $26 < r_s < 67$ in three dimensions and for $13 < r_s < 33$ in two dimensions, and the normal or unpolarized fluid is stable at higher densities, $r_s < 26$ in three dimensions and $r_s < 13$ in two dimensions. A pseudopotential with no adjustable parameters, derived from the random-phase approximation, is found to give excellent energies. The present results lend support to earlier conjectures that the ground state of the electron gas will be spin polarized at intermediate densities.

III. VARIATIONAL TRIAL FUNCTION

In this paper we will assume the trail function is of the Bijl-Dingle-Jastrow[14] or product form:

$$\Psi_T(R) = D(R) \exp\left(-\sum_{i<j}^{N} u(|\vec{r}_i - \vec{r}_j|)\right). \qquad (4)$$

The function $D(R)$ is the "model" noninteracting term and serves to give the trail function the desired antisymmetry. For the fluid phase we take $D(R)$ to be a Slater determinant of plane waves. In the unpolarized fluid there are separate determinants for spin-up and spin-down particles. For the polarized fluid there is a single determinant. In the crystal phase $D(R)$ is a Slater determinant of single-particle orbitals centered around the lattice sites. The "pseudopotential," $u(r)$ is repulsive and includes in an approximate way the effects of particle correlation.

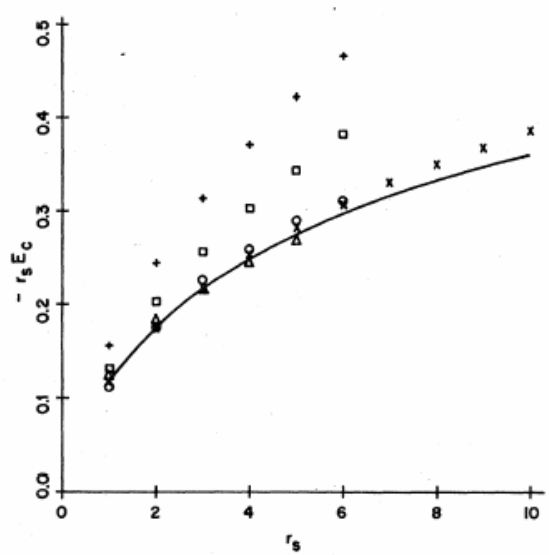

FIG. 2. Minus the correlation energy times r_s vs r_s from our calculation (solid line) compared with perturbational calculations. The symbols represent the results of (+) the RPA approximation Freeman (Ref. 41), (□) Hubbard (Ref. 45), (○) Vashishta and Singwi (Ref. 43), (×) Freeman (e^s) (Ref. 41), and (△) Lowy and Brown (Ref. 44).

Ground State of the Electron Gas by a Stochastic Method

D. M. Ceperley

National Resource for Computation in Chemistry, Lawrence Berkeley Laboratory, Berkeley, California 94720

and

B. J. Alder

Lawrence Livermore Laboratory, University of California, Livermore, California 94550

(Received 16 April 1980)

An exact stochastic simulation of the Schroedinger equation for charged bosons and fermions has been used to calculate the correlation energies, to locate the transitions to their respective crystal phases at zero temperature within 10%, and to establish the stability at intermediate densities of a ferromagnetic fluid of electrons.

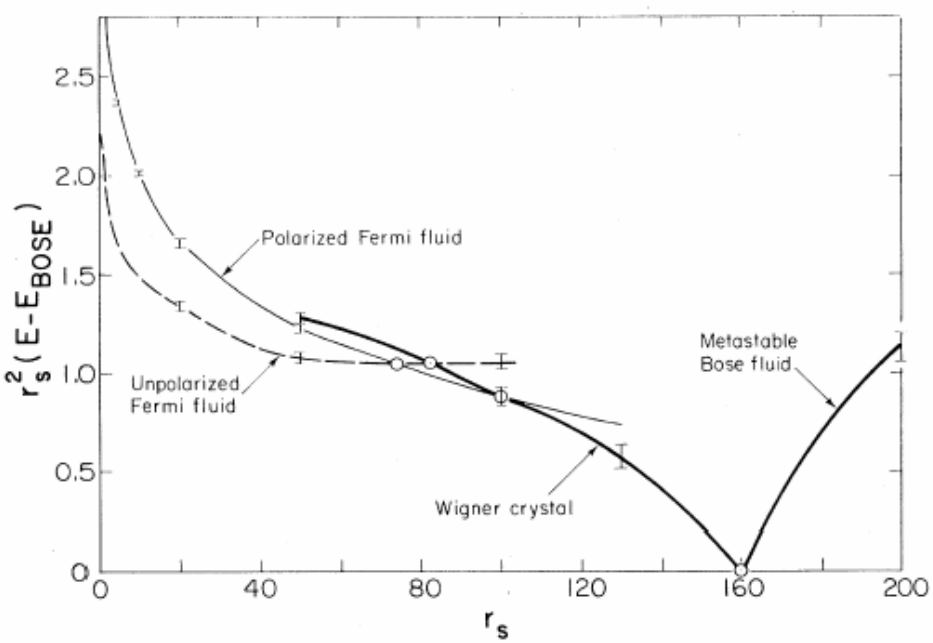

FIG. 2. The energy of the four phases studied relative to that of the lowest boson state times r_s^2 in rydbergs vs r_s in Bohr radii. Below $r_s = 160$ the Bose fluid is the most stable phase, while above, the Wigner crystal is most stable. The energies of the polarized and unpolarized Fermi fluid are seen to intersect at $r_s = 75$. The polarized (ferromagnetic) Fermi fluid is stable between $r_s = 75$ and $r_s = 100$, the Fermi Wigner crystal above $r_s = 100$, and the normal paramagnetic Fermi fluid below $r_s = 75$.

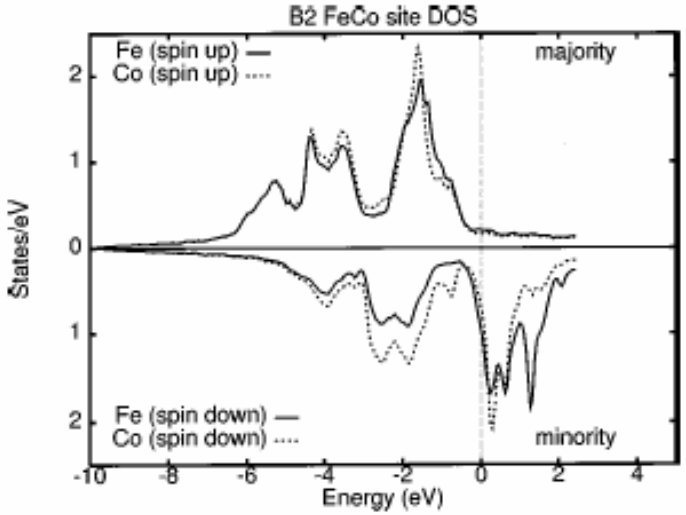

FIG. 3. Spin-resolved density of states for the Fe and Co sites in ordered α' ($B2$-based) FeCo.

A "strong ferromagnet" has essentially filled majority band and partially filled minority band. (Ni, FeCo alloys)

A "weak ferromagnet" has partially filled majority as well as minority band. (Fe, Co)

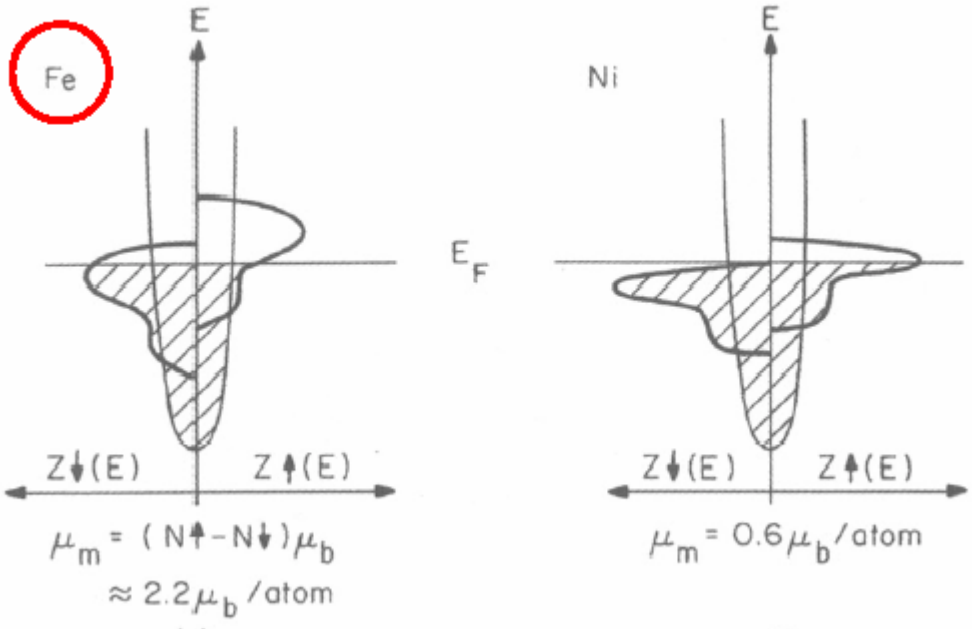

Definitions:

Paramagnet **weak ferrom.** **strong ferrom.**

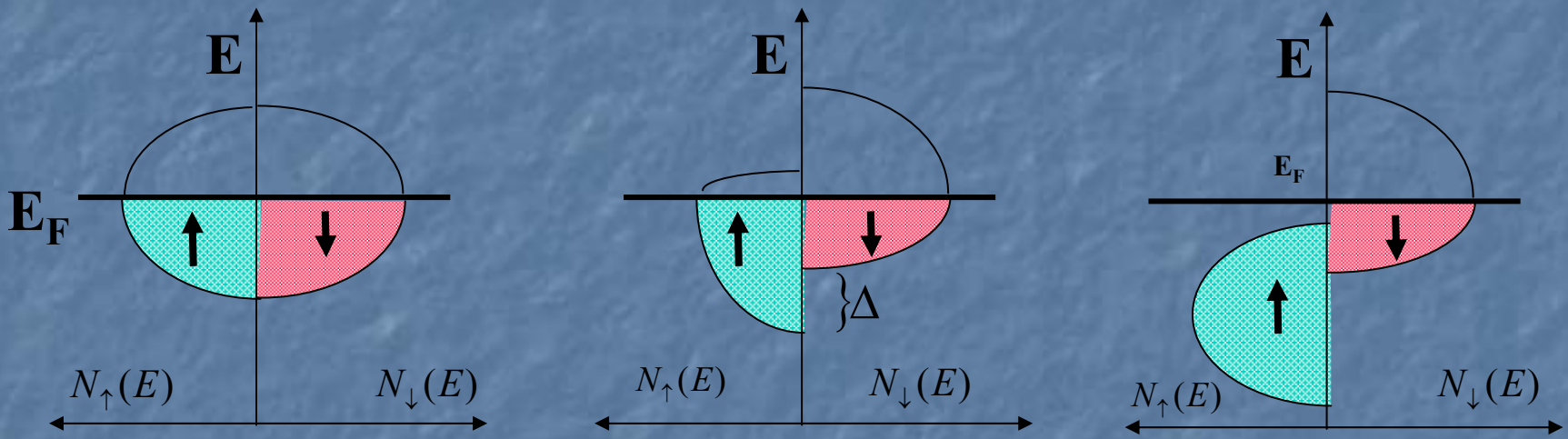

no polarisation **partially polarized** **fully pololarized**

Ti, V **Fe, Co** Ni

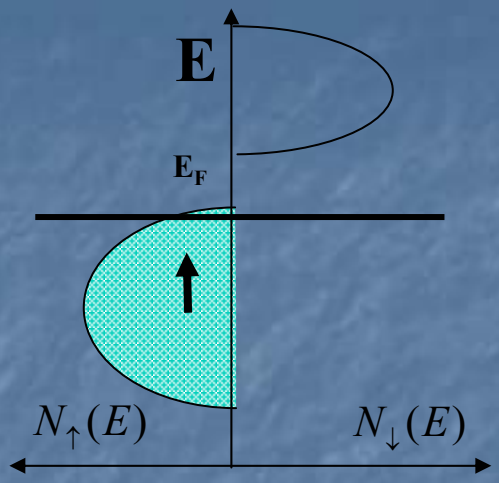

Half metallic alloy with full polarisation:

Examples:

ferromagnetic oxide CrO2 and some intermetallic compounds (Heusler-alloys) PtMnSb, NiMnSb, Co2MnAl, Co2MnSb.

LDA Local Density Functional theory and its applications in Magnetism: Numerical procedure based on the Kohn Sham scheme and the Hohenberg Kohn variational principle

PHYSICAL REVIEW B VOLUME 38, NUMBER 10 1 OCTOBER 1988

Stoner model of ferromagnetism and total-energy band theory

P. M. Marcus and V. L. Moruzzi
IBM Research Division, Thomas J. Watson Research Center, P.O. Box 218, Yorktown Heights, New York 10598
(Received 7 March 1988)

The Stoner model of ferromagnetism in metals is generalized to reproduce the results of spin-polarized total-energy band calculations with the fixed-spin-moment procedure. The Stoner parameter for the exchange field is made a function of both volume and magnetic moment and evaluated from the band calculations. A generalized Stoner condition for the occurrence of ferromagnetism is derived and applied to fcc Fe. Our previous results on the high-spin and low-spin phases of fcc Fe are reproduced and differences from a recent Stoner analysis of fcc Fe are explained.

$$\chi^{-1}(M,V)=\frac{\partial^2\Delta E_T(M,V)}{\partial M^2}$$

$$=\frac{1}{2\bar{N}}-\frac{M}{2\bar{N}^2}\bar{N}'-\frac{I}{2}-MI'-\frac{M^2}{4}I'' , \quad (3.10)$$

where $\bar{N}'=(\partial\bar{N}/\partial M)_V$, $I'=(\partial I/\partial M)_V$, $I''=(\partial^2 I/\partial M^2)_V$. Then

$$\chi(0)=\frac{2\bar{N}(0,V)}{1-\bar{N}(0,V)I(0,V)}=\frac{2N(\varepsilon_F,V)}{1-N(\varepsilon_F,V)I(0,V)} . \quad (3.11)$$

The spin-polarized Kohn-Sham equations may be written[5]

$$(-\nabla^2+\phi_{\text{eff}\,j}(n_u(\mathbf{r}),n_d(\mathbf{r})))\psi_{ij}(\mathbf{r})=\varepsilon_{ij}\psi_{ij}(\mathbf{r}) ,$$
$$i=1,2,\ldots,N_j \text{ and } j=u,d , \quad (2.1)$$

where u and d designate up- and down-spin distributions, respectively, and the effective potential is

$$\phi_{\text{eff}\,j}(n_u(\mathbf{r}),n_d(\mathbf{r}))=\phi_{\text{Coul}}(\mathbf{r})+\phi_{\text{xc}\,j}(n_u(\mathbf{r}),n_d(\mathbf{r})) , \quad (2.2)$$

and the Coulomb part is the sum of a nuclear and an electronic part

$$\phi_{\text{Coul}}(\mathbf{r})\equiv\phi_{\text{nuc}}(\mathbf{r})+\phi_{\text{elec}}(\mathbf{r})$$
$$=\sum_p \frac{Z_p}{|\mathbf{r}-\mathbf{R}_p|}+\int_V \frac{n(\mathbf{r}')}{|\mathbf{r}-\mathbf{r}'|}d^3r' , \quad (2.3)$$

with the electron number density for each spin

$$n_j(\mathbf{r})=\sum_{i=1}^{N_j} |\psi_{ij}(\mathbf{r})|^2, \quad j=u,d , \quad (2.4)$$

and the total electron number density

$$n(\mathbf{r})=\sum_{j=u,d} n_j(\mathbf{r}) . \quad (2.5)$$

In (2.3), $\mathbf{R}_p$ is the lattice vector of the nucleus of charge Z_p and the sum is over all nuclei. In (2.2)

$$\phi_{\text{xc}\,j}=\frac{\partial[n\varepsilon_{\text{xc}}(n_u,n_d)]}{\partial n_j}, \quad j=u,d , \quad (2.6)$$

where $\varepsilon_{\text{xc}}(n_u,n_d)$ is a known function in the local-density approximation.[6] The equations (2.1) are solved self-consistently under the two constraints

$$\int_V n_j(\mathbf{r})d^3r=N_j, \quad j=u,d , \quad (2.7)$$

where N_u and N_d are specified separately and the total number of electrons per atom is

$$N=\sum_{j=u,d} N_j . \quad (2.8)$$

If the system is neutral, N is fixed by the Z values and only the difference

$$M=N_u-N_d \quad (2.9)$$

can vary; M is then the magnetic moment of the system in Bohr magnetons.

The total energy of the system is a function of M and of the set of nuclear coordinates $\{\mathbf{R}_p\}$, and is given by

$$E_T(M,\{\mathbf{R}_p\})=\sum_{j,i}\varepsilon_{ij}-\tfrac{1}{2}\int_V n(\mathbf{r})\phi_{\text{elec}}(\mathbf{r})d^3r$$
$$+\int_V\left[n(\mathbf{r})\varepsilon_{\text{xc}}(\mathbf{r})-\sum_j n_j(\mathbf{r})\phi_{\text{xc}\,j}(\mathbf{r})\right]d^3r . \quad (2.10)$$

This doubly constrained self-consistent ground-state calculation, which fixes both N and M, is called the fixed-spin moment procedure.[7] For cubic bulk crystals it leads to a thermodynamic function $E_T(M,V)$, which contains information about the stable and metastable ferromagnetic bulk phases and their stability ranges in V. We note

TABLE I. Theoretical equilibrium lattice constants a_{theo} (in a.u.), spin magnetic moments (in μ_B) and total hyperfine field B_{tot} (in kG) as well as their core and valence parts, B_{cor} and B_{val}, for bcc Fe, fcc Co, and fcc Ni, respectively. In addition the decomposition of B_{cor} into its contributions from the $1s$, $2s$, and $3s$ shells is given. The last line represents the ratio of the core hyperfine field B_{cor} and the spin magnetic moment μ_{spin} in kG/μ_B, respectively. As explained in the text the abbreviations VBH and so on denote the various parametrizations for the used exchange-correlation potentials. All results have been obtained assuming a nucleus of finite radius r_n with r_n=8.22, 8.33, and 8.44×10^{-5} a.u. for Fe, Co, and Ni, respectively. The corresponding experimental values for the lattice constant are 5.406, 6.707, and 6.658 a.u., 2.13 μ_B, 1.52 μ_B and 0.57 μ_B for the magnetic moment and −339, −215, and −75 kG for the total hyperfine field, respectively.

(a) Fe

	VBH	JWM	VWN	LM-JWM	PW-JWM	PW-VWN	GGA91	EV93
a_{theo}	5.245	5.270	5.263	5.344	5.511	5.496	5.438	5.774
μ_{spin}	2.09	2.18	2.16	2.34	2.54	2.50	2.46	2.87
B_{1s}	−18	−18	−19	11	7.5	7.2	−7.4	13
B_{2s}	−479	−513	−508	−620	−481	−474	−590	−937
B_{3s}	284	293	298	327	270	275	317	504
B_{cor}	−213	−238	−229	−305	−203	−192	−280	−420
B_{val}	−9.4	−13	−14	−5.6	−36	−39	−36	15
B_{tot}	−222	−250	−243	−311	−239	−231	−316	−405
$B_{\text{cor}}/\mu_{\text{spin}}$	−102	−109	−106	−130	−80	−77	−114	−146

(b) Co

	VBH	JWM	VWN	LM-JWM	PW-JWM	PW-VWN	GGA91	EV93
a_{theo}	6.533	6.559	6.550	6.631	6.798	6.790	6.715	7.076
μ_{spin}	1.53	1.60	1.59	1.66	1.71	1.70	1.68	1.89
B_{1s}	−16	−17	−17	−11	5.6	5.5	−6.8	8.0
B_{2s}	−396	−425	−420	−497	−382	−380	−461	−714
B_{3s}	249	260	262	283	246	250	272	412
B_{cor}	−163	−182	−175	−225	−131	−125	−196	−294
B_{val}	−65	−59	−62	−50	−32	−34	−44	−11
B_{tot}	−228	−241	−237	−275	−163	−159	−240	−305
$B_{\text{cor}}/\mu_{\text{spin}}$	−106	−114	−110	−136	−77	−74	−117	−155

(c) Ni

	VBH	JWM	VWN	LM-JWM	PW-JWM	PW-VWN	GGA91	EV93
a_{theo}	6.533	6.549	6.543	6.623	6.802	6.795	6.715	7.080
μ_{spin}	0.60	0.62	0.61	0.64	0.63	0.63	0.63	0.75
B_{1s}	−7.5	−7.8	−7.8	−5.0	2.3	2.2	−3.2	3.3
B_{2s}	−170	−179	−178	−210	−162	−161	−191	−323
B_{3s}	111	114	115	125	112	113	119	191
B_{cor}	−67	−73	−71	−90	−48	−45	−76	−128
B_{val}	−17	−16	−16	−16	−13	−13	−15	−12
B_{tot}	−83	−89	−87	−106	−60	−59	−91	−140
$B_{\text{cor}}/\mu_{\text{spin}}$	−112	−117	−116	−140	−76	−71	−121	−171

8.44×10^{-5} a.u. for Fe, Co, and Ni, respectively. The corresponding experimental values for the lattice constant are 5.406, 6.707, and 6.658 a.u., 2.13 μ_B, 1.52 μ_B and 0.57 μ_B for the magnetic moment and −339, −215, and −75 kG for the total hyperfine field, respectively.

LDA and the Transition metals.

Phys Rev B53, 9776 (96)

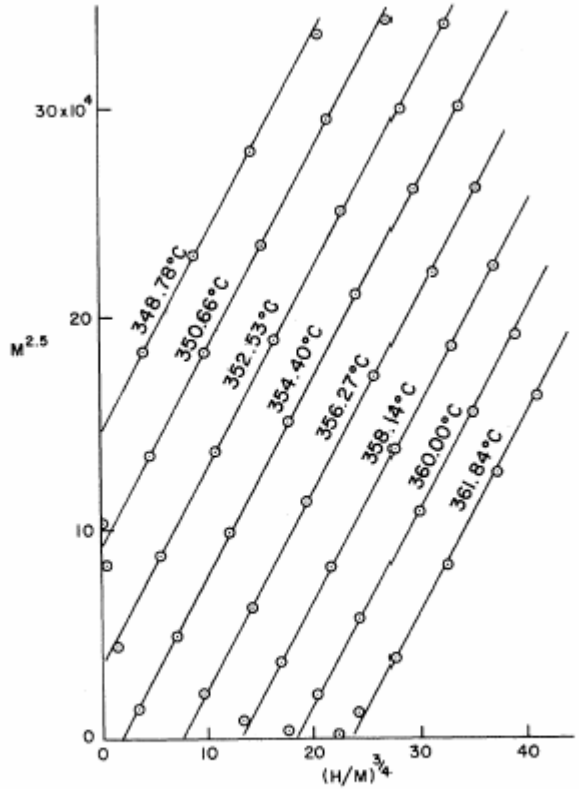

FIG. 3. A replot of the data of Weiss and Forrer to conform to the variables of Eq. (1).

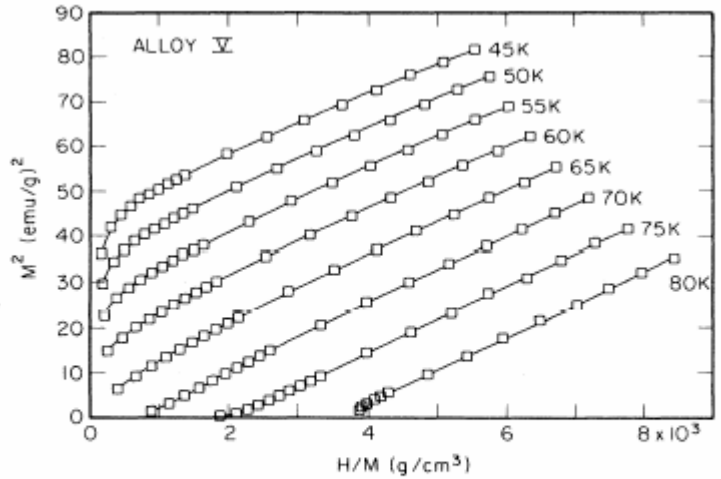

FIG. 2. Arrott plots for alloy V at eight temperatures between 45 and 80 K.

PHYSICAL REVIEW B VOLUME 40, NUMBER 17 15 DECEMBER 1989-I

Low-temperature behavior of Ni_3Al alloys near the spin-fluctuator–ferromagnet phase boundary

S. K. Dhar,* K. A. Gschneidner, Jr., L. L. Miller, and D. C. Johnston
Ames Laboratory, Departments of Materials Science and Engineering and of Physics, Iowa State University, Ames, Iowa 50011
(Received 5 July 1989)

Arrott Noakes: Ni (1967 PRL)

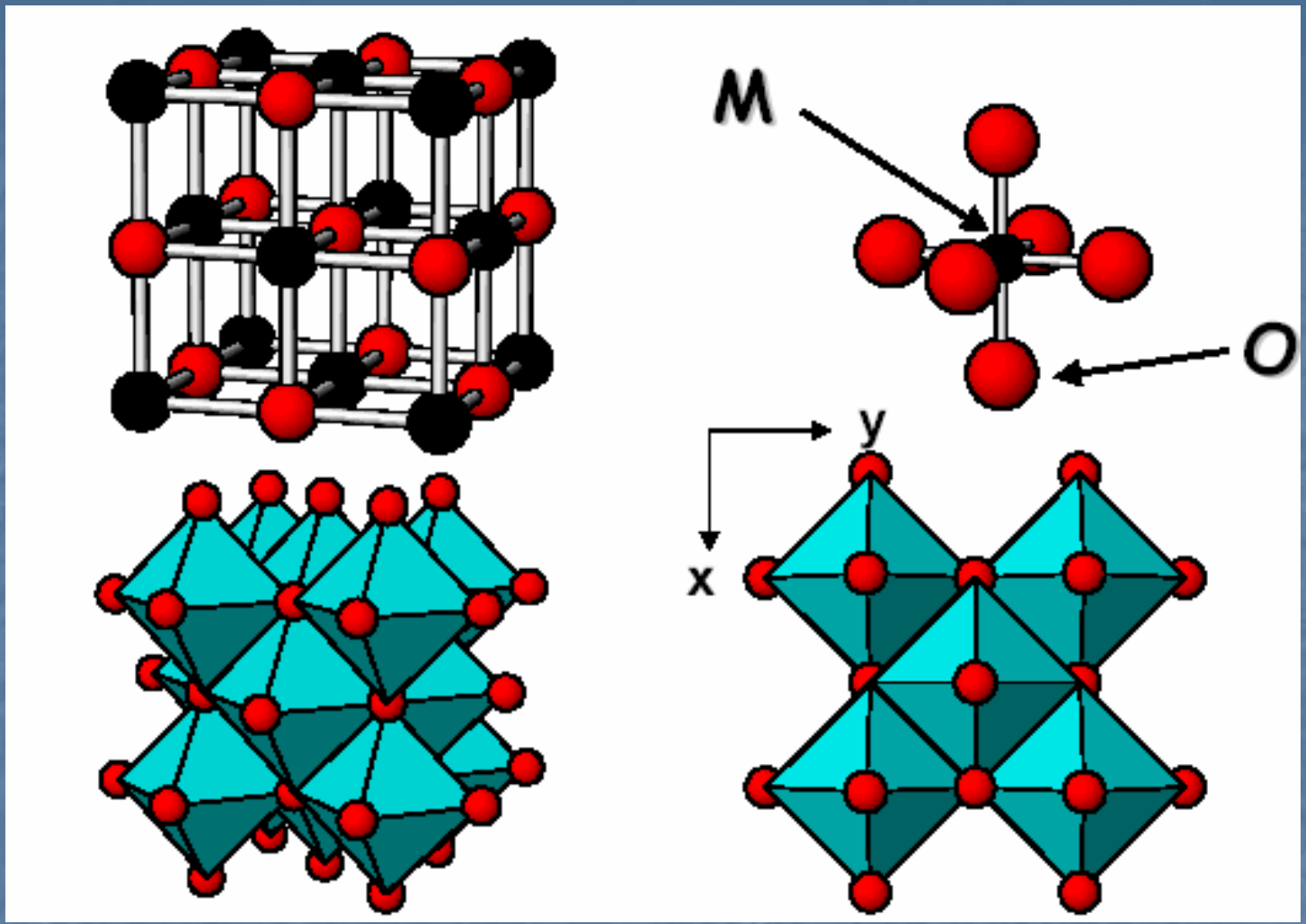

Na Cl structure of MO, where M= transition metal.

Note the M surrounded by O octahedra.

3d Transition Metal Monoxides

Compound	M-M Distance	Electrical Properties	Magnetic Properties
TiO (d^2)	2.94 Å	Metallic	Pauli Paramagnetic
VO (d^3)	2.89 Å	Intermediate	Intermediate
MnO (d^5)	3.14 Å	Semiconductor	AFM T_N = 122 K
FeO (d^6)	3.03 Å	Semiconductor	AFM T_N = 198 K
CoO (d^7)	3.01 Å	Semiconductor	AFM T_N = 293 K
NiO (d^8)	2.95 Å	Semiconductor	AFM T_N = 523 K

AFM = Antiferromagnetic

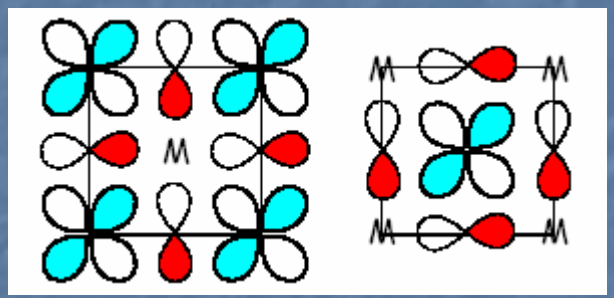

Example of t_2g overlap with oxygen p levels

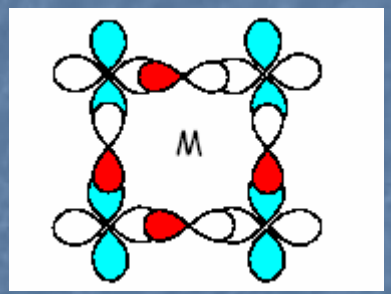

Example of e.g. overlap of Cu d levels with oxygen p levels